

# **Fine-scale analysis of shelf –slope physiography across the western continental margin of India**

Bishwajit Chakraborty\*, Ranadhir Mukhopadhyay, Pratima Jauhari,  
Vasudev Mahale, K Shashi Kumar, Rajesh M.

*National Institute of Oceanography, Dona Paula 403 004, Goa, INDIA*

*Abstract:* We attempt here to quantify and model physiographic phenomena off the central west coast of India in terms of power spectral exponent, amplitude parameter. The statistical analysis of the multibeam echosounder grid bathymetry data is able to characterise the outer shelf, upper slope, shelf margin basin, and several structural rises. The scatter diagram analysis shows that the seafloor can be grouped in two distinct clusters. Distinctly different clustering patterns are observed over the structural rises compared to shelf, slope, basinal areas. This may suggest different modes of formation for the members of these two clusters. In fact, the steep and sharply elevated structural rises appear to be part of NW-SE trending coast parallel Mid-Shelf Basement and Prathap ridges. These ridges are rift-induced volcanic emplacements on a stretched and thinned continental crust which probably formed during mid- Cretaceous times.

*\* communicating author*

*e-mail address: [bishwajit@nio.org](mailto:bishwajit@nio.org)*

*fax number: 00-91-832-2450609*

*telephone number: 00-91-832-2450318*

## **Introduction**

The western continental margin of India (WCMI) is a zone of extensional tectonics of the lithosphere, and of interactions between continental and oceanic crust. The WCMI is considered to represent a passive margin which largely developed during two main periods, i.e. between 89 to 84 Ma BP when India got separated from Madagascar, being accentuated by sub-surface magma convection from the Marion hotspot, and between 68 to 60 Ma BP when the Seychelles, Saya de Malha, and the Laxmi Ridge became detached from India in association with eruptions of the Reunion hotspot and subsequent seafloor spreading along the Carlsberg Ridge (Naini and Talwani 1983; Storey et al. 1995; Todal and Eldholm 1998; Reeves and de Wit 2000).

We present a fine-scale analysis of the seafloor and several geomorphic features from a small portion of the outer shelf and shelf margin basin in the upper slope area off the central west coast of India (Fig. 1). The study area includes nine structural rises ranging in height from 400 m to more than 1800 m water depth and a valley in the south. We have estimated the spectral exponent, amplitude and fractal dimension values to quantify variations in seafloor morphology (Mandelbrot; 1983; Barenblatt et al. 1984). In the spectral analysis, the derived amplitude of the Fourier transformed output shows a power law dependence on wave number (Welch 1967). During the study, we employed the spectral technique to understand seafloor complexities. We model these geomorphic features using gridded multi-beam bathymetric data to shed light on their evolution by estimating seafloor roughness associated with their power law exponent and fractal dimensions. Within the framework of regional tectonics, the model suggests more than one mode of formation for these geological features.

## **Materials and methods**

### *Study area and data acquisition*

An area close to 20,500 km<sup>2</sup> was surveyed off the central west coast of India during two expeditions onboard Ocean Research Vessel (ORV) Sagar Kanya (SK-65 and SK-158). The bathymetry data was collected from the outer shelf to upper slope area lying between 11.8°N to 15.5°N latitude and 72.3°E to 74.3°E longitudes using a multibeam (MB) Hydrosweep echosounder operating at 15.5 kHz frequency (Fig. 1). In this region, the shelf break is located about 105 km from the coast, followed by a 116 km wide shelf margin basin. A roughly 13 km wide Mid-Shelf Basement Ridge divides the basin into an about 30 km wide eastern and an about

73 km wide western basin (Chaubey et al. 2002). An igneous intrusive complex (Prathap Ridge) runs through the centre of the western basin (Naini and Talwani 1983; Subrahmanyam et al. 1995). The two ridges lie about 37-40 km apart. The study (survey) area encompasses a gently sloping outer shelf, the eastern part of the shelf margin basin, and five structural rises located on a Mid-Shelf Basement Ridge, and another four rises on the Prathap Ridge in the western basin. The Mid-Shelf Basement Ridge is visibly the dominant feature in the basin, whereas the Prathap Ridge is largely covered with sediment except for areas with peaks and rises (Chaubey et al. 2002; Krishna, personal communication).

In this study area, seafloor depth varies from shallow (~64 m) to deep (~2200 m) areas, and it is difficult to obtain evenly spaced raw data from echo-sounding system. In order to obtain evenly spaced data the raw bathymetry data was manually cleaned and gridded using spline-interpolation (grid cell size 100 m) to plot contour maps and to extract depth profiles using Generic Mapping Tool (GMT) (Douds, 1998). We extracted several evenly spaced depth-grid profiles; namely profiles A, B, and D on the outer shelf, E along the shelf-break, profiles C, F, and G over the Mid-Shelf Basement Ridge, and profile H over the Prathap Ridge in the shelf margin basin (Fig. 1). The Digital Terrain Model (DTM) of the survey area also served the purpose of suitable visualization (Fig. 2). Moreover, in order to determine the spectral parameters in the east-west directions, data at regular intervals were estimated from seven short profiles (I - O) across the structural rises and floor of the shelf margin basin.

Anisotropic characteristics of the seafloor were studied at ten locations having good two-dimensional data coverage (locations a to j, Fig. 1). For each of these locations, nine bathymetric profiles were extracted from the grid at a regular angular interval of 22.5° degrees while going round from North (0°) to South (180°). Length of the profiles is varying from 7 km to 26 km. Directions and lengths of the nine profiles at each location is indicated by arrows (Fig. 1).

### *Fine-scale analysis*

We used a spectral technique to obtain model parameters for sea floor topography (Berkson and Mathews 1983; Chakraborty et al 2003). Since the spectral technique was developed primarily for the treatment of stationary data, we separated non-stationary data into stationary intervals before the spectral parameters were estimated (Malinverno 1989). The power spectral density function is obtained using a smoothed periodogram approach (Welch 1967). The input profile is

de-trended to remove the best-fit linear trend of the original profile. Then the first and last 10% of each profile is tapered with a  $\cos^2$ - function to minimize the edge effect or leakage (Goff and Jennings 1999). A Fast Fourier Transform (FFT) algorithm is then applied, and the resulting complex spectrum is squared to achieve a sample power spectrum periodogram.

The results are then plotted into  $\log_{10}$ - $\log_{10}$  plots. The power law equation [ $\log_{10} P_H = (-\beta) \log_{10} f + \log_{10} c$ ] is represented on a logarithmic scale. Comparing this with a straight-line equation, ‘ $\beta$ ’ corresponds to the slope of a straight line fitted to the power spectrum and the intercept ‘ $c$ ’ of the input profile. In the present case, the true drop in power occurs somewhere around wavelengths  $\sim 3$  to  $\sim 40$ km (Goff and Jennings 1999). In the estimation of power law parameter ( $\beta$ ) along each profile, the percentage error is estimated to vary within 1.4% to 6.4% for the entire dataset. We employed a window length [ $\log_{10}$  (wave number)] varying from  $\sim -0.8$  to  $0.35$ , which is similar to values applied in other studies (Goff and Jennings 1999). For a one-dimensional topographic profile, the fractal dimension is estimated from the spectral exponent  $\beta$  as [ $D = (5 - \beta) / 2$ ]. Fig. 3 (a) shows depth profile ‘C’ and estimated ‘ $\beta$ ’ values along with the segmented sections. Fig. 3 (b) presents Power spectral density versus wave number for the first segment of the profile ‘C’ and estimated ‘ $\beta$ ’ value by use of curve fitting.

The first-order segmentation was made using root mean square (rms) value of the profile (Fox and Hayes 1985). However, we used the power law parameter  $\beta$  and the amplitude parameter  $S$  here (e.g., Malinverno 1989). For segmentation, it is necessary to design an algorithm that will separate a given non-stationary profile into a series of segments whose statistical characteristics are reasonably homogeneous. As mentioned earlier, the amplitude parameter ‘ $S$ ’ of a profile, which is required for the segmentation, is given as [ $S = 1.4826 * MAD$ ] where  $MAD$  is the median of the absolute deviation from the sample median (Malinverno 1989). To estimate fine-scale seafloor variations, the selected 15 profiles (A to H and I to O) were divided into 35 segments,- i.e. eight segments in the eastern basin, twenty-three across structural rises of the Mid-Shelf Basement Ridge (6, 8 and 9 segments each), and four segments in the western basin over the Prathap Ridge.

Moreover, in order to determine study parameters related to seafloor anisotropy analyses of the nine mini profiles of each of the ten spot (a to j) are carried out. For every profile belonging to a particular location, the spectral parameter ( $\beta$ ) and intercept ( $a$ ) is estimated. The estimated

intercept parameters are plotted with respect to the azimuth angles ( $0^\circ$  to  $180^\circ$ ), and a sinusoidal curve fitting technique is employed for each location to obtain amplitude of the sinusoid parameter ( $v$ ). Also for each location, azimuth of maximum energy ( $\theta$ ), and average of the intercept ( $a^1$ ) and slope of the spectrum ( $\beta_{\text{mean}}$ ) are obtained.  $\theta$ , is presented in Fig. 1.

## Results

The spectral analyses, supported by the digital terrain model of the study area which varies in depth between 64 and 2200m, show a gently sloping continental outer shelf, a steep continental upper slope (eastern and western parts of shelf margin basins), nine structural rises of variable height and a canyon-like-depression in the south (Fig. 2). Of the nine bathymetric highs, five are major (summit heights  $> 1000\text{m}$ , Rises 01, 03, 04, 08 and 09), two are large (summit height 500-999 m, Rises 02 and 05), and two are small (summit height 100- 499 m, Rises 06 and 07). Of these, Rises 02, 03, 06, and 07 are located on Prathap Ridge, whereas the rest are located along the Mid-Shelf Basement Ridge. The structural rises on the Prathap Ridge are pointed and conical, whereas those over the Mid-Shelf Basement ridge have smooth flat-topped summits. The summit heights (m), summit areas ( $\text{km}^2$ ), and ranges in flatness (summit / basal area) of the major structural rises are, Rise 01: 1650 m,  $254 \text{ km}^2$ , 7.17-9.40; Rise 03: 1400 m,  $8 \text{ km}^2$ , 5.42-19.11; Rise 04: 1500 m,  $9.5 \text{ km}^2$ , 5.7-11.14; Rise 08: 1550 m,  $76 \text{ km}^2$ , 6.57-9.47; and Rise 09: 1000 m,  $154 \text{ km}^2$ , 5.34-8.39.

The estimated ' $\beta$ ' and ' $D$ ' values of the thirty-five segmented sections are found to vary between 4.70 and 0.51, and 0.13 and 2.25 respectively. Overall, the ' $\beta$ ' values are always negative with large magnitudes (low ' $D$ ' values), representing terrains which are relatively rough at large scales and smooth at smaller scales. Conversely, lower magnitudes of the ' $\beta$ ' parameter (and higher ' $D$ ' value) represent terrains which are smoother at large scales than at small scales. The fractal dimension value of the largely even eastern basin (i.e., devoid of flanks and highs), by contrast lie well within the fractal limits. Again, the estimated fractal dimension values ( $D$ ) along the relatively short east-west trending profiles I to O are also well within the fractal limits (1.08-1.43). The area is relatively smooth without any sharp deviation in depth. The estimated fractal dimensions ( $D$  values) of several segments along the profiles from various depths of the slopes do not fulfill the required fractal criteria for 1-dimensional data ( $1.0 > D < 2.0$ ), and will not be considered for analysis of the present physiographic provinces.

The scatter diagram between the power spectral exponent ( $\beta$ , instead of fractal dimension  $D$ ) and amplitude ( $S$ ) parameters offers interesting results (Fig. 4). The overall roughness observed in the study area groups in two distinct clusters. Cluster A includes variations in all the structural rises, including the five major ones (Rise 01, 03, 04, 08 and 09) and smaller one (Rise 07). These areas show high  $S$  and low to moderate  $\beta$ , suggesting seafloor roughness on a large scale. In contrast to this, Cluster B comprises the remainder of the areas, including the gently sloping outer shelf and the eastern and part of the western shelf margin basins. The seafloor here shows low to moderate  $S$  and moderate to high  $\beta$ , suggesting dominantly small-scale undulations.

The average anisotropy values of the estimated parameters [ $\beta_{\text{mean}}$ ,  $a^1$ ,  $v$ , and  $\theta$ ] from mini profiles of each of the ten spot (a to j) are illustrated in Fig. 5. The parameters ' $v$ ' and ' $a^1$ ' represents degree of anisotropy of the surface, and overall roughness of the terrain respectively. For a and b locations, the parameters: ' $v$ ' and ' $a^1$ ' are comparatively higher than the other eight locations. A gradual fall in  $\beta_{\text{mean}}$ , is observed starting from locations a to j.

## **Discussion**

A comparison of the clustering of the nine structural rises (cluster A) with that of the outer continental shelf and basin regions (cluster B, Fig. 4) may indicate differences in their mode of origin (volcanic and plutonic, respectively). For example, the Mid-Shelf Basement Ridge and the Prathap Ridge (including their manifestation by nine structural rises) are believed to have been formed by emplacement of volcanic material during the separation of India and Madagascar in mid-Cretaceous times (Agarwal et al. 1992; Subrahmanyam et al. 1995; Todal and Eldholm 1998). The process of rifting started with clockwise rotation and trans-tensional rifting between the two continental masses represented by a wedge of extended and stretched continental crust about 200 km wide and which is presently preserved as the western continental shelf of India (Todal and Eldholm 1998; Reeves and de Wit 2000). Critical observation of the clustered pattern of these rises (cluster A; Fig. 4) indicates the difference in the positions of the scatter data points (H1 and H3) of the profile H (Fig. 2). Profile H lies along the Prathap Ridge and provides four segments. H1 and H3 are the rise (03 and 07 respectively). In general, relative shift in the positions of the remaining scatter points for structural rises along the profiles C, F and G from Mid-Shelf Basement Ridge is observed while comparing with profile H. Such differences may be due to the rifting of two landmasses (India and Madagascar), which is often accompanied by massive igneous activities. It is possible that the Marion plume then-located beneath this rift

experienced extensive decompression melting due to crustal stretching and thinning (Storey et al 1995). The melt rose from Marion plume during 89–85Ma and surfaced through several rifts running parallel to the contact of these two landmasses (Storey et al 1995; Kumar et al. 2001). Such volcanic eruption is believed to form Mid-Shelf Basement Ridge, the Prathap Ridge, and the structural rises located along them.

The summits of the major structural rises are extremely flat and smooth, and are similar to the outer shelf and floor of the shelf margin basin. The outer shelf and floor of the eastern basin show extremely low amplitudes ( $S \sim 0.08\text{-}0.51\text{m}$ ), but variable spectral exponent values ( $\beta \sim 0.75\text{-}3.77$ ). When excluding deeper segments of the outer shelf profiles (A, B and top- upper slope E), we obtain spectral exponent values within the 0.75- 2.03 limit (Fig. 2 and 5). Similar results from the summits of some of the major rises show low amplitudes ( $S \sim 0.71\text{-}1.72\text{m}$ ) and low spectral exponents ( $\beta \sim 0.508\text{-}2.070$ ). This similarity in spectral exponent and amplitude values of the shallower part of the outer shelf, the floor of the eastern basin, and the summits of the rises may suggest prominence of sub-aerial erosion (Naini and Talwani 1983; Subrahmanyam et al. 1995). This interpretation, however, requires independent confirmation.

The ability of the method employed here, including the distribution of azimuths of maximum energy ( $\theta$ ), to quantify seafloor roughness and anisotropy introduces interesting possibilities for geological investigations. For example,  $\theta$  is oriented towards the south along the Prathap Ridge (spots d, e, h). By contrast,  $\theta$  over the Mid-Shelf Basement Ridge is largely oriented towards the north and northeast (spots f, i, j, b, g; Fig. 1). This difference in  $\theta$  distribution is reflected by an apparent structural shift of minor scale between the two (Fig. 2). This NNW-SSE offset of minor scale may also have a bearing on the formation of nearby canyon-like depressions. Detailed magnetic studies may throw light on this conjecture in future. To examine the broader adaptability of our method, these values are compared with those from the fast accreting Gorda Rise spreading center in the Pacific Ocean. The mean amplitude ( $a'$ ), amplitude of the sinusoid ( $v$ ), and azimuth of maximum energy ( $\theta$ ) for the study area (a) are 0.81 m, 0.39 m and  $135^\circ$  respectively as compared to 1.68 m, 0.51 m, and  $115^\circ$ , respectively, for the Gorda Rise (Fox and Hayes 1985). This indicates that the study area ('a') is 52% less isotropic and 24% less anisotropic as compared to those in the Gorda Rise area. Relatively low mean intercept values ( $a^1$ ) in the study area are indicative of a smoother seafloor than observed in the Gorda Rise

spreading center. Distinct seafloor roughness patterns from these two very different structural regimes illustrate the ability of the method to detect variable seafloor morphology at finer scales.

**Acknowledgements:** The Department of Ocean Development, New Delhi supported this research through grant for the EEZ project (GAP 1438 under MLP 0014). We thank VN Kodagali, B Theerthesh and R Madhupriya for timely help. This is NIO contribution 4124.



## Caption to the Figures

### Fig. 1

Gridded multibeam bathymetric data (100m contour interval) from the study area. Profiles A-H were used for segmentation and spectral parameter estimation, and I to O are taken on track plot C and G. Segmented sections for each profiles are numbered along the profiles. Data from locations 'a' to 'j' and symbol (\*) indicates nine profiles chosen for anisotropy study. The length of the nine profiles from each spot is varying from 9 -26 km (indicated by sizes of the selected nine profiles from each spot). Arrows indicate azimuths of maximum energy ( $\theta$ ), and numbers (01-09) denote structural rises. No contours on the profile D is seen due to its lower depth (much lower than the 100m throughout the profile).

### Fig. 2

Digital Terrain Model and 3D-perspective view of the study area [scale 1: 500,000, and vertical height exaggeration 70 x]. Structural rises are numbered (01-09). Two compass directions are shown N-S, E-W. View plan is tilted 20° from the horizontal towards the -z direction.

### Fig. 3

- a) Segmented depth data along with  $\beta$  (slope) values.
- b) Power spectral density versus wave number for the first segment for profile C is given as an example.

### Fig. 4

Estimation of power law parameters ' $\beta$ ' (slope) and ' $S$ ' (amplitude) of the segmented data. Note two clusters; A : structural rises and B : outer shelf and basinal regions.

### Fig. 5

Relationship between mean slope ( $\beta_{\text{mean}}$ ) (right hand side axis), mean intercept amplitude ( $\mathbf{a}'$ ), and amplitude of sinusoid ( $\mathbf{v}$ ) (left hand side axis) from ten locations (cf. Fig. 1).

## References

- Agarwal PK, Pandey OP, JG Negi (1992) Madagascar: A continental fragment of the paleo-super Dharwar craton of India. *Geology* 20:543-546
- Barenblatt GI, Zhivago AV, Neprochnov YP, Ostrovskiy AA (1984) The fractal dimension: A quantitative characteristic of ocean bottom relief. *Oceanology* 24:695-697
- Berkson JM, JE Matthews (1983) Statistical properties of seafloor roughness. In: Pace NG Acoustic in the Sea-Bed (Ed): Bath Univ Press, Bath, pp 215-223
- Chakraborty B, VN Kodagali, J Baracho (2003) Seafloor classification using multibeam echosounding angular backscatter data: A real time approach employing hybrid neural network architecture. *IEEE JOE* 28:121-128
- Chaubey AK, D Gopala Rao, K Srinivas, T Ramprasad, MV Ramana, V Subrahmanyam (2002) Analyses of multichannel seismic reflection, gravity and magnetic data along a regional profile across the central-western continental margin of India. *Mar Geol* 182:303-323
- Douds ASB (1998) Fractal analysis of topography and structure across the Appalachian foreland of West Virginia. M.S. Thesis, West Virginia University, pp 115
- Fox CG, DE Hayes (1985) Quantitative methods for analyzing the roughness of the seafloor. *Rev Geophys* 23:1-48
- Goff KA, JW Jennings Jr (1999) Improvement of Fourier-based unconditional and conditional simulations for band limited fractal (von Karman) statistical models. *Math Geol* 31:627-649
- Kumar A, K Pande, TR Venkatesan, and YJ Bhaskar Rao (2001) The Karnataka Late Cretaceous dykes as products of the Marion hotspot at the Madagascar-India breakup event: evidence from  $^{40}\text{Ar}/^{39}\text{Ar}$  geochronology and geochemistry. *Geophys Res Lett* 28:2715-2718

Malinverno A (1989) Segmentation of topographic profiles of the seafloor based on a self-affine model. IEEE JOE 14-4:348-359

Mandelbrot BB (1983) The Fractal Geometry of Nature. Freeman, New York, pp 468

Naini BR, M Talwani (1983) Structural framework and the evolutionary history of the continental margin of western India. In: Watkins JS, Drake CL (eds) Studies in continental margin geology. AAPG Memoir 34:167-191

Reeves C, M de Wit (2000) Making ends meet in Gondwana: retracing the transforms of the Indian Ocean and reconnecting continental shear zones. Terra Nova 12:272-280

Storey M, JJ Mahoney, AD Saunders, RA Duncan, SP Kelley, MF Coffin (1995) Timing of hotspot related volcanism and the break-up of Madagascar and India. Science 267:852-855

Subrahmanyam V, MV Ramana, D Gopala Rao, KS Krishna, GPS Murty, M Gangadhara Rao (1995) Structure and tectonics of the southwestern continental margin of India. Tectonophysics 249:267-282

Todal A, O Eldholm (1998) Continental margin of western India and Deccan Large Igneous Province. Mar Geophy Res 20:273-291

Welch PD (1967) The use of fast Fourier transform for the estimation of power spectra: A method based on time averaging over short, modified periodograms. IEEE Trans Audio Electroacoust AU-15:70-73

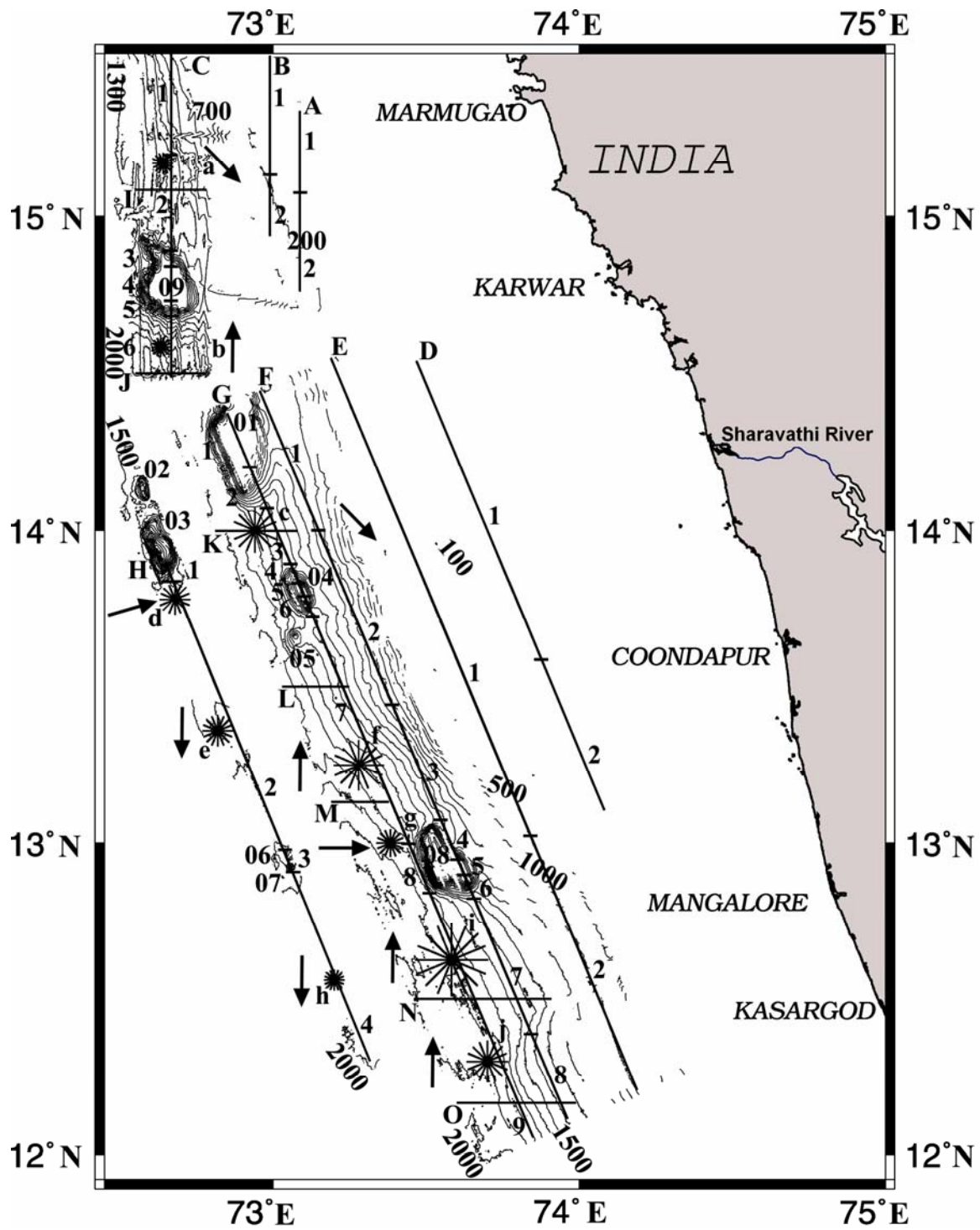


Fig. 1

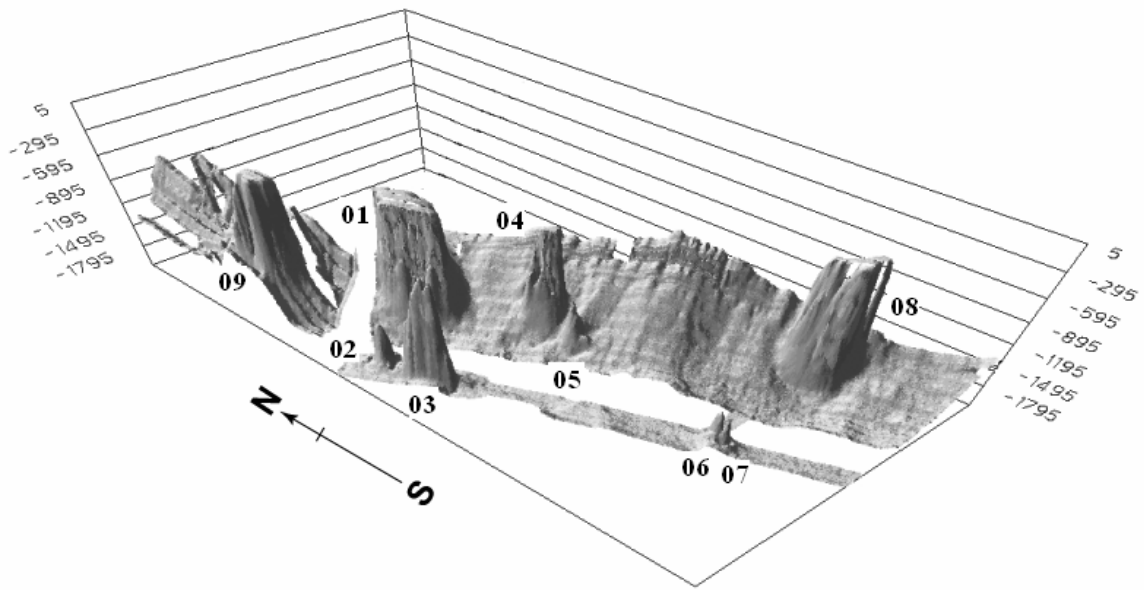


Fig. 2

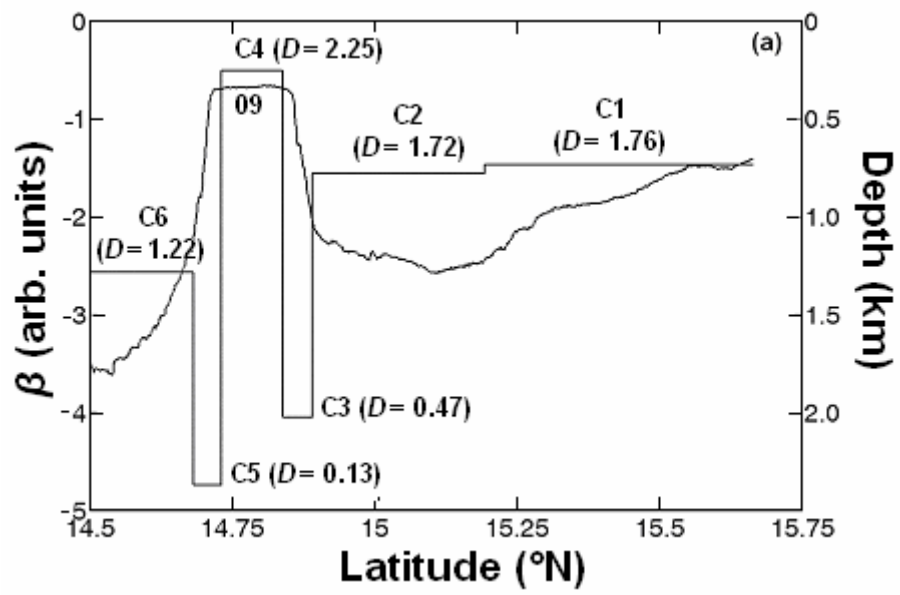


Fig. 3a

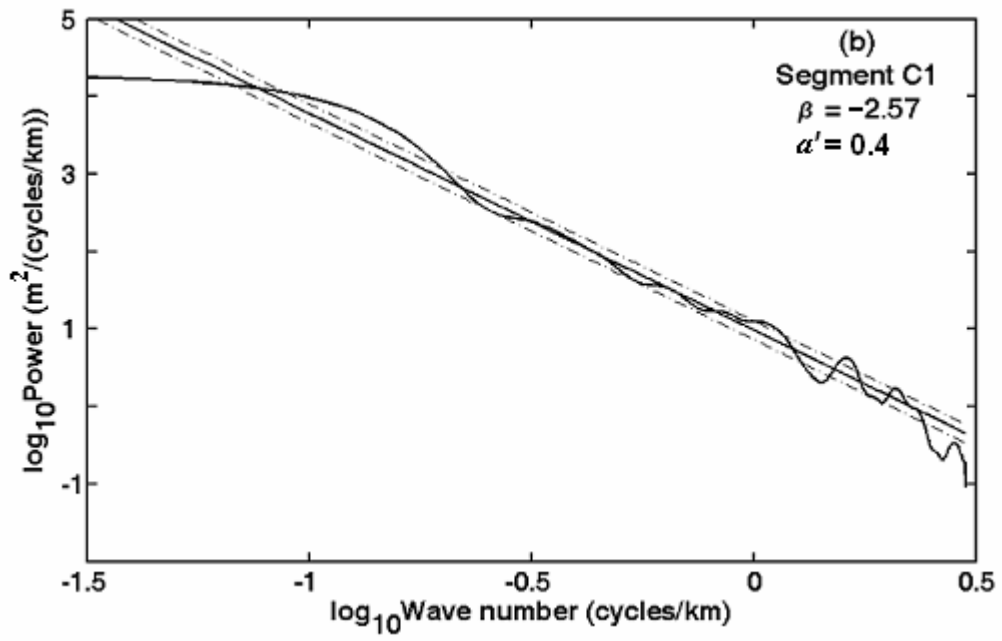


Fig. 3b

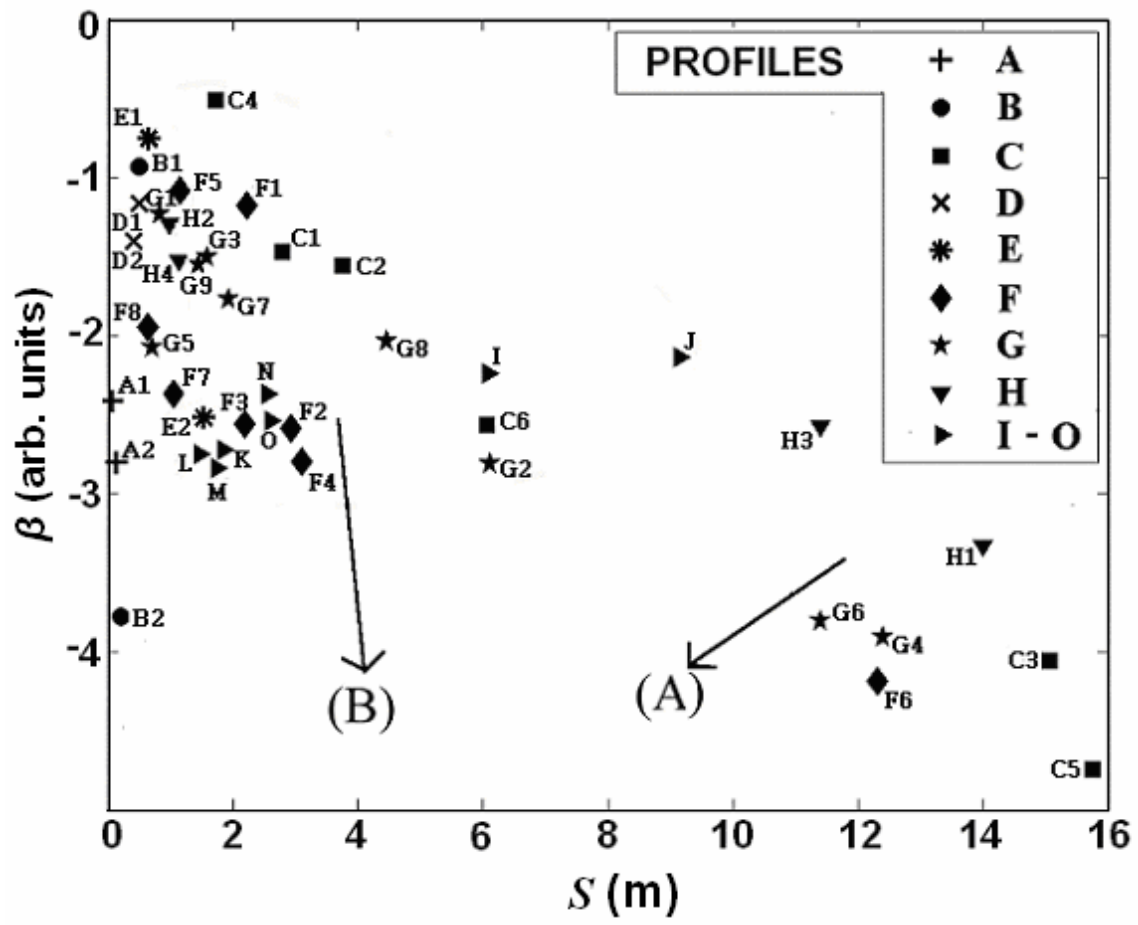


Fig. 4



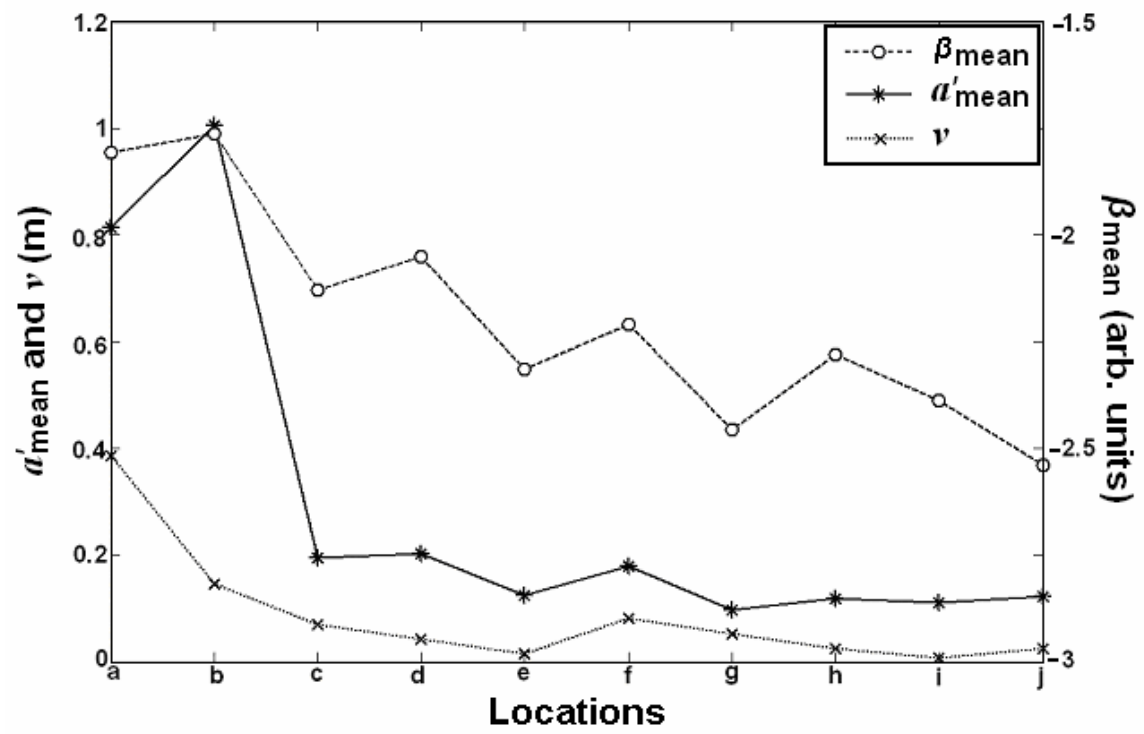


Fig. 5